Biochimica et Biophysica Acta 1820 (2012) 1062–1072

Contents lists available at SciVerse ScienceDirect

Biochimica et Biophysica Acta

journal homepage: www.elsevier.com/locate/bbagen

Characterization of dual effects induced by antimicrobial peptides: Regulated cell death or membrane disruption

Edgar J. Paredes-Gamero [a,b,*,1], Marta N.C. Martins [b,1], Fábio A.M. Cappabianco [c], Jaime S. Ide [c], Antonio Miranda [b,*]

[a] Departamento de Bioquímica, Universidade Federal de São Paulo, R. Três de Maio 100, 04044-020, São Paulo, SP, Brazil
[b] Departamento de Biofísica, Universidade Federal de São Paulo, R. Três de Maio 100, 04044-020, São Paulo, SP, Brazil
[c] Departamento de Ciência e Tecnologia, Universidade Federal de São Paulo, R. Talim, 330, 12231-280, São José dos Campos, SP, Brazil

ARTICLE INFO

Article history:
Received 23 November 2011
Received in revised form 17 February 2012
Accepted 24 February 2012
Available online 7 March 2012

Keywords:
Antimicrobial peptide
Cell death
Membrane permeabilization
Intracellular mechanism

ABSTRACT

Background: Some reports describe lysis mechanisms by antimicrobial peptides (AMPs), while others describe the activation of regulated cell death. In this study, we compare the cell death-inducing activities of four β-hairpin AMPs (gomesin, protegrin, tachyplesin and polyphemusin II) along with their linear analogs in the human erythroleukemia K562 cell line to investigate the relationship between their structure and activity.
Methods: K562 cells were exposed to AMPs. Morphological and biochemistry alterations were evaluated using light microscopy, confocal microscopy and flow cytometry.
Results: Gomesin and protegrin displayed cytotoxic properties that their linear counterparts did not. Tachyplesin and polyphemusin II and also their linear analogs induced cell death. We were able to distinguish two ways in which these AMPs induced cell death. Lower concentrations of AMPs induced controlled cell death mechanisms. Gomesin, tachyplesin and linear-tachyplesin promoted apoptosis that was characterized by annexin labeling, sensitivity to Z-VAD, and caspase-3 activation, but was also inhibited by necrostatin-1. Gomesin and protegrin induced cell death was dependent on intracellular Ca^{2+} mechanisms and the participation of free radicals was observed in protegrin induced cell death. Polyphemusin II and its linear analog mainly induced necrosis. Conversely, treatment with higher concentrations of AMPs primarily resulted in cell membrane disruption, but with clearly different patterns of action for each AMP tested.
Conclusion: Different actions by β-hairpin AMPs were observed at low concentrations and at higher concentrations despite the structure similarity.
General significance: Controlled intracellular mechanism and direct membrane disruption were clearly distinguished helping to understand the real action of AMPs in mammalian cells.

1. Introduction

The limited number of chemotherapeutic drugs available on the market for use against cancer cells led to a frantic search for new compounds. In recent years, several antimicrobial peptides (AMPs) have been described as molecules with potential anti-cancer activity [1–6]. AMPs are present in nearly all organisms displaying diverse tridimensional structures. In general, AMPs are cationic, amphipathic and with molecular weights of less than 10 kDa [7].

Studies performed in bacteria indicate that the main action of AMPs involves the formation of membrane pores [8–11]. Conversely, studies in mammalian cells have shown that AMPs may promote cell death by apoptosis, autophagy or necrosis. For instance, magainin, a cationic and amphipathic α-helix peptide, induces cell death by apoptosis in HL-60 cells [12]. Tachyplesin, a peptide with a disulfide bridge that forms a stabilized amphipathic β-hairpin structure [4], induces apoptosis in HL-60 cells [13] but promotes membrane permeabilization in a prostate carcinoma cell line [4]. Gomesin, another β-hairpin AMP, presents high cytotoxic activity against cancer and normal cells by regulating membrane permeabilization [1], although it also triggers a complex intracellular Ca^{2+} signaling pathway prior to membrane permeabilization [14]. In a hepatocellular carcinoma, peptaibols, a family of antibiotic peptides from fungi, have been demonstrated to suppress tumor growth by inducing Ca^{2+} influx. This effect on Ca^{2+} influx in turn leads to the activation of μ-calpain and promotion of Bax translocation to the mitochondria, triggering apoptosis and autophagy, suggesting less evidence for a mode of action via membrane permeabilization [2]. There are few reports comparing how the structures and activities of AMPs induce cell death in mammalian cells.

* Corresponding authors at: Departamento de Bioquímica, Universidade Federal de São Paulo, R. Três de Maio, 100, 04044-020, São Paulo, SP, Brazil. Tel.: +55 11 5576 4442; fax: +55 11 5573 6407.
E-mail addresses: edgar.gamero@unifesp.br (E.J. Paredes-Gamero), amiranda@unifesp.br (A. Miranda).
[1] These authors contributed equally to this work.

0304-4165
doi:10.1016/j.bbagen.2012.02.015

Herein, we compare the ability of four β-hairpin AMPs (tachyplesin, gomesin, polyphemusin II and protegrin) to induce cell death, distinguishing whether cellular actions are different among them. We also tested their corresponding linear (Lin) analogs and also magainin II, a linear AMP. β-Hairpin AMPs such as tachyplesin and polyphemusin II display antitumoral ability against leukemia cells [13,15]. Therefore, in this study the human erythroleukemia K562 cell line was used as cellular model to investigate the effects of these AMPs. Herein, we were able to distinguish diverse effects among β-hairpin AMPs. We observed that at concentrations below the EC_{50} AMPs promoted cell death by different intracellular mechanisms depending on the AMP used, and at concentrations above the EC_{50}, AMPs induced diverse types of membrane disruptions.

2. Experimental procedures

2.1. Peptide synthesis

Peptides were synthesized manually by the solid-phase method on a 4-methylbenzhydrylamine-resin (MBHAR) (0.8 mM/g) using the *t*-Boc strategy [16]. Full deprotection and cleavage of the peptide from the resin were carried out using anhydrous hydrogen fluoride (HF) treatment with anisole and dimethyl sulfide (DMS) as scavengers at 0 °C for 1.5 h. Formation of disulfide bridges was achieved immediately after the HF cleavage and extraction of the crude peptide. The resulting peptide solution was kept at pH 6.8–7.0 and 5 °C for 72 h. Cyclization reactions were monitored by reverse-phase liquid chromatography coupled to an electrospray ionization mass spectrometer (LC/ESI-MS). Lyophilized crude peptides were purified by preparative RP-HPLC on a Vydac C_{18} column (25 × 250 mm, 300 Å pore size, and 15 μm particle size) in two steps. The first was performed by using triethylammonium phosphate (TEAP) pH 2.25 as solvent A and 60% acetonitrile (ACN) in A as solvent B. The second step was carried out using 0.1% trifluoroacetic acid (TFA) H_2O as solvent A and 60% ACN in A as solvent B. Pure peptides were characterized by amino acid analysis and by LC/ESI-MS. The sequences of the AMPs are shown in Table 1.

2.2. Cell line and culture conditions

A K562 erythroleukemia cell line obtained from the American Type Culture Collection (ATCC, USA), was cultured in suspension in RPMI 1640 medium (Cultilab, Brazil) supplemented with 10% fetal calf serum (FBS, Cultilab, Brazil), 100 U/ml of penicillin, and 100 μg/ml of streptomycin in a humidified atmosphere at 37 °C in 5% CO_2.

2.3. Cell viability assay

Cells were seeded in 96-well plates (10^5 cells/ml) and cultured in medium containing 10% FBS in the presence or absence of AMPs for 24 h. After this period, K562 cells were washed with PBS and resuspended in binding buffer (0.01 M Hepes, pH 7.4, 0.14 M NaCl and 2.5 mM $CaCl_2$). The suspensions were labeled with annexin-FITC and propidium iodide (PI) (Becton Dickinson, USA) according to the manufacturer's instructions. The cells were incubated at room temperature for 20 min. 10,000 events were collected per sample. The analysis was performed in a FACSCalibur flow cytometer (Becton Dickinson, USA) using the CellQuest software (Becton Dickinson, USA).

2.4. Caspase-3 activity

K562 cells were treated with the AMPs as indicated, and activation of caspase-3 was evaluated by flow cytometry according to the manufacturer's instructions (Cell Signaling, USA). After treatment, K562 cells were centrifuged, washed and fixed in 2% paraformaldehyde in PBS for 30 min. Cells were then permeabilized in PBS containing 0.01% saponin for 15 min and blocked in PBS containing 1% BSA for 30 min at room temperature. Afterwards, 10 μl of cleaved caspase-3 (Asp175) Alexa Fluor 488-conjugated antibody was added, and cells were incubated in the dark at room temperature for 1 h. After washing, cells were resuspended in PBS and analyzed (10,000 events collected per sample) in a FACSCalibur flow cytometer (Becton Dickinson, USA) using the CellQuest software.

Table 1
Sequence and cytotoxicity activities of the peptides.

Peptides	Sequences	MW	EC_{50}[a] (μM)
Magainin	**G-I-G-K-F-L-H-S-A-K-K-F-G-K-A-F-V-G-E-I-M-N-S-NH$_2$**	2465.95	>40
Gomesin	**Z-C-R-R-L-C-Y-K-Q-R-C-V-T-Y-C-R-G-R-NH$_2$**[b]	2270.72	4.5
[Trp^1,$Ser^{2,6,11,15}$]-Gomesin or Lin-gomesin	**W-S-R-R-L-S-Y-K-Q-R-S-V-T-Y-S-R-G-R-NH$_2$**	2285.62	>40
Tachyplesin	**K-W-C-F-R-V-C-Y-R-G-I-C-Y-R-R-C-R-NH$_2$**	2263.78	20
[Trp^0,$Ser^{3,7,12,16}$]-Tachyplesin or Lin-tachyplesin	**W-K-W-S-F-R-V-S-Y-R-G-I-S-Y-R-R-S-R-NH$_2$**	2389.76	21
Polyphemusin II	**R-R-W-C-F-R-V-C-Y-K-G-F-C-Y-R-K-C-R-NH$_2$**	2425.97	22
[Trp^0,$Ser^{4,8,13,17}$]-Polyphemusin II or polyphemusin II	**W-R-R-W-S-F-R-V-S-Y-K-G-F-S-Y-R-K-S-R-NH$_2$**	2551.95	22
Protegrin	**R-G-G-R-L-C-Y-C-R-R-R-F-C-V-C-V-G-R-NH$_2$**	2155.64	12
[Trp^0,$Ser^{6,8,13,15}$]-Protegrin or Lin-protegrin	**W-R-G-G-R-L-S-Y-S-R-R-R-F-S-V-S-V-G-R-NH$_2$**	2281.64	>40

[a] Cytotoxicity activities of the AMPs were evaluated against K562 erythroleukemia cell line.
[b] Z = pyroglutamic acid residue.

2.5. DNA content

Cells were treated with the indicated AMPs for 24 h. After this period, cells were washed, fixed and permeabilized as described previously. Then, cells were treated with 4 μg/ml RNase type I for 1 h at 37 °C and resuspended in PBS. Cells were stained with 5 μg/ml PI and analyzed (12,000 events collected per sample) in a FACSCalibur flow cytometer using the CellQuest software. The DNA content was evaluated using a FL2H detector on a logarithmic scale. The analysis of the cell percentage in the sub-G_0/G_1 phase was performed using the Winmdi 2.8 software.

2.6. ROS measurement

Levels of hydrogen peroxide were determined using 5-(and-6)-chloromethyl-2′,7′-dichlorodihydrofluorescein diacetate (CM-H_2DCFDA; Invitrogen, USA). Treated cells were incubated with 10 μM CM-H_2DCFDA for 30 min and washed with PBS. Fluorescent signals were detected by flow cytometry.

2.7. Ca^{2+} measurement

Intracellular Ca^{2+} was measured using confocal microscopy equipped with a Plan-Apochromat 63× objective lens (Numerical aperture 1.4) (Zeiss, LSM 780, Germany). K562 cells were incubated with 4 μM Fluo-4/AM for 30 min at room temperature, and then washed with Hank's Buffered Salt Solution (HBSS; composition in mM: 137 NaCl, 5.4 KCl, 0.25 Na_2HPO_4, 0.44 KH_2PO_4, 1.3 $CaCl_2$, 1.0 $MgSO_4$, 4.2 $NaHCO_3$). Fluo-4 was excited with an argon laser (λ_{Ex} = 488 nm), and light emission was detected using a Zeiss META detector (λ_{Em} = 500–550 nm). The pinhole device was not used. Images were collected at approximately 5 s intervals. Fluorescence intensity was normalized to basal fluorescence levels using Examiner 3.2 (Zeiss, Germany) and Image J (USA) software [17,18].

2.8. Photomicrographic analysis

The Nikon Advanced Modulation Contrast method was used to take photomicrographs. Photomicrographs of cultured cells were obtained using a Nikon DS-Fi1 digital camera mounted on a Nikon TS100 phase contrast microscope equipped with an Achro LWD NAMC 40× objective lens (Numerical aperture 0.55) (Nikon Instruments, USA).

2.9. Confocal microscopy

Nuclear evaluation was assessed by analysis of DNA binding to PI. After treatment with AMPs, cells were fixed and permeabilized as

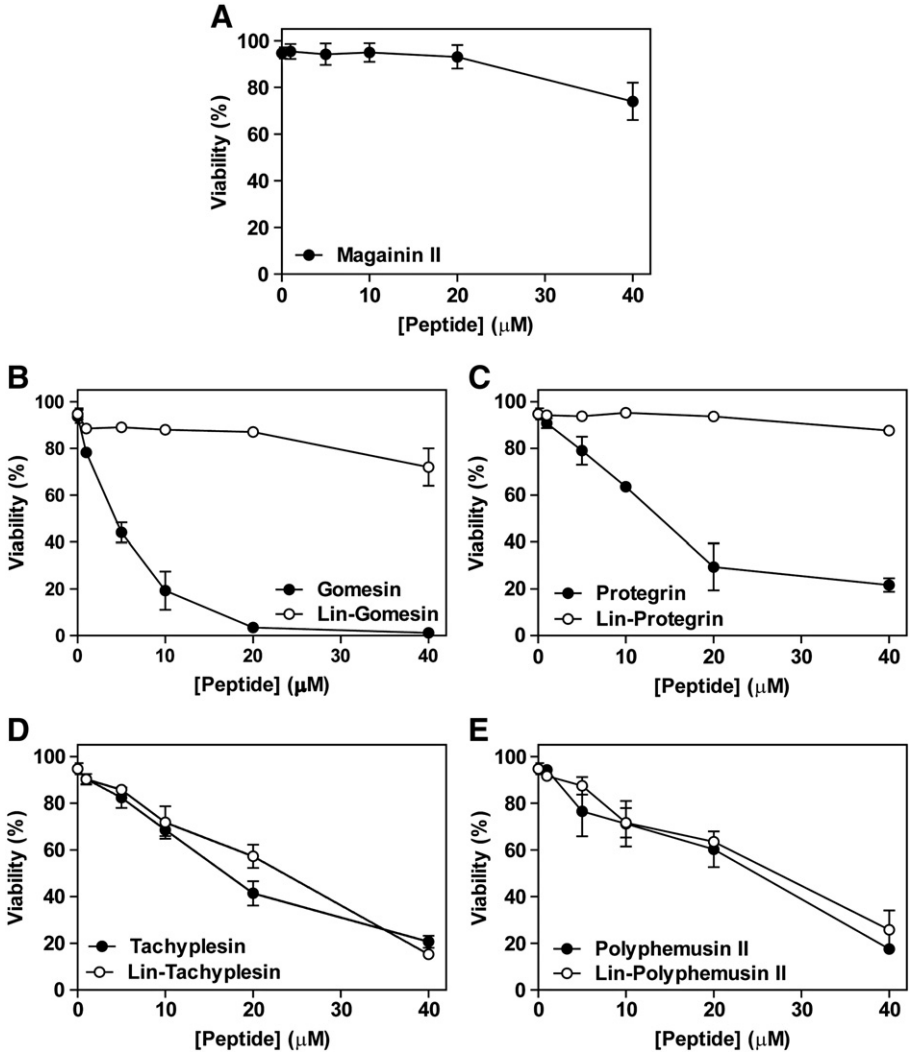

Fig. 1. Cytotoxicity curves of AMPs in K562 cells. K562 cells were treated with different concentrations of AMPs for 24 h, and then evaluated. Cell viability was determined using annexin-V and PI staining following treatment with (A) magainin, (B) gomesin and Lin-gomesin, (C) protegrin and Lin-protegrin, (D) tachyplesin and Lin-tachyplesin, and (E) polyphemusin and Lin-polyphemusin. Results are the means ± SEM of three independent experiments performed in duplicate.

described previously. After washing in PBS, cells were incubated with PI for 15 min. After incubation, cells were placed onto glass coverslips and mounted with Fluoromount-G.

The cellular membrane of K562 cells was labeled with 4 μg/ml Alexa Fluor 488-conjugated wheat germ agglutinin (WGA) for 30 min and fixed. Then, cells were placed onto glass coverslips and mounted with Fluoromount-G.

Microscopy analyses were performed with a confocal laser scanning microscope. The pinhole device was adjusted to capture fluorescence of one airy unit in one focal section, and several Z stacks were captured to analyze the total cellular volume. Images were obtained using an argon laser ($\lambda_{Ex} = 488$ nm), and the emitted fluorescence was detected from 500 nm to 550 nm using a META detector (Zeiss, Germany).

2.10. Statistical analysis

The Fluo-4 fluorescence intensity was normalized to basal intensity (F_t/F_0) and is shown as a representative pseudo-colored image according to a fluorescence intensity scale ranging from 0 (black) to 255 (white) [18]. All data represent at least three independent experiments and were expressed as mean ± standard error of the mean (SEM). Statistical analyses were performed using Student's t-test for comparison between two groups, and analysis of variance (ANOVA) and Dunnett's post hoc test for multiple comparisons among groups. A probability value of $P<0.05$ was considered significant.

3. Results

3.1. AMPs induce apoptosis, secondary necrosis, necrosis and necroptotic cell death

To compare the cytotoxic abilities of AMPs against K562 erythroleukemia cell line, we employed annexin and PI assay. Annexin-V is a protein that binds to phosphatidylserine that becomes exposed to extracellular cell membrane during apoptosis, and PI is a nuclear stain that is impenetrant to viable cells [19]. Thus, annexin and PI staining make it possible to differentiate between viable cells (PI^-An^-), apoptotic cells (PI^-An^+), necrotic cells (PI^+An^-) and secondary necrosis of cells (PI^+An^+). Magainin II (an α-helical AMP), four β-hairpin AMPs (gomesin, protegrin, tachyplesin and polyphemusin II), and their linear counterparts (Lin-gomesin, Lin-protegrin, Lin-tachyplesin and Lin-polyphemusin II) were used in this study. Linear analogs of β-hairpin AMPs were constructed by replacing Cys by Ser at the position indicated in Table 1.

Magainin II displayed reduced cytotoxic activity in K562 cells up to a concentration of 40 μM (Fig. 1A). Gomesin and protegrin were the most potent cytotoxic AMPs in K562 cells, but their corresponding linear analogs, Lin-gomesin and Lin-protegrin, lost their cytotoxic activity (Fig. 1B and C). Tachyplesin and polyphemusin (Fig. 1D and E) and notably, their linear analogs were cytotoxic for K562 cells (Fig. 1D and E). A comparison of the cytotoxic activities of the AMPs used in this study is shown in Table 1.

We observed differences in the mode of cell death depending on the concentration of AMPs that correlated to their EC_{50} values. Gomesin, the most potent AMP, primarily induced apoptosis in K562 cells (Fig. 2A), while tachyplesin and its linear counterpart promoted cell death primarily by apoptosis and secondary necrosis (Fig. 2B). Protegrin, polyphemusin II and its linear analog mainly induced secondary necrosis and necrosis (Fig. 2C and D).

To corroborate the effects described above, caspase inhibitor Z-VAD was used. Cells were incubated with the inhibitor for 1 h before the addition of AMPs. Z-VAD was able to reduce gomesin, tachyplesin and Lin-tachyplesin induced cell death, whereas the cell death, which involves a high percentage of secondary necrosis or necrosis, induced by protegrin, polyphemusin II and Lin-polyphemusin II was not affected (Fig. 3A). In addition, the activity of caspase-3 in the presence of AMPs was evaluated. Caspase-3 is an effector caspase that plays an important role in the execution phase of apoptosis [20]. Among the peptides tested, gomesin and tachyplesin were able to produce the cleaved active form of pro-caspase-3, confirming that gomesin and tachyplesin induce apoptosis in K562 cells (Fig. 3B).

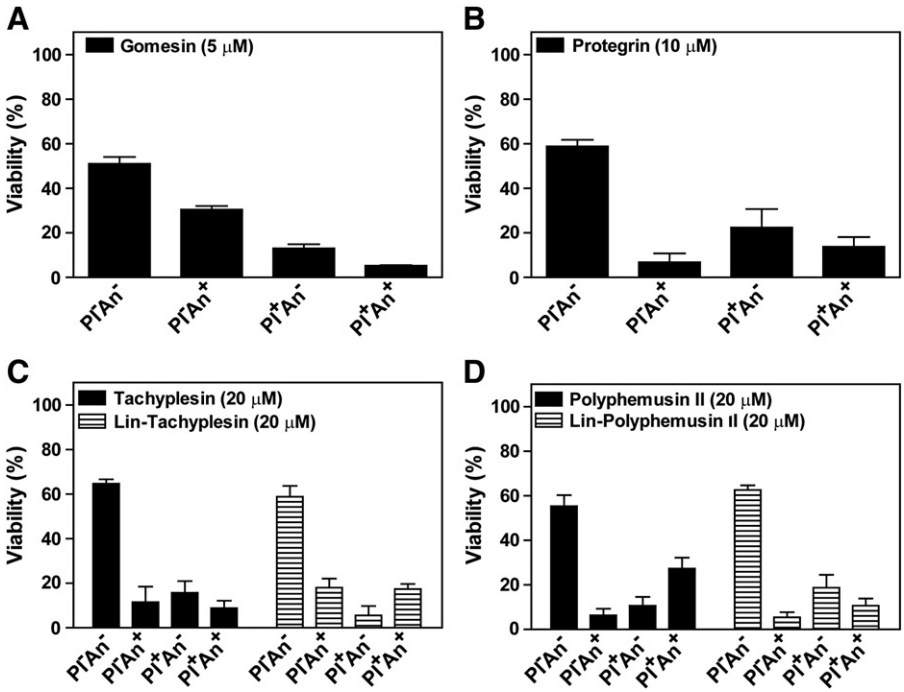

Fig. 2. The cytotoxic effects of AMPs occur via different modes of cell death. The type of cell death induced by AMPs was evaluated by flow cytometry analysis using annexin-V and PI staining. Results are presented as the percentage of viable (PI^-An^-), apoptotic (PI^-An^+), secondary apoptotic (PI^+An^+) and necrotic (PI^+An^-) cells. Results are the means ± SEM of three independent experiments performed in duplicate.

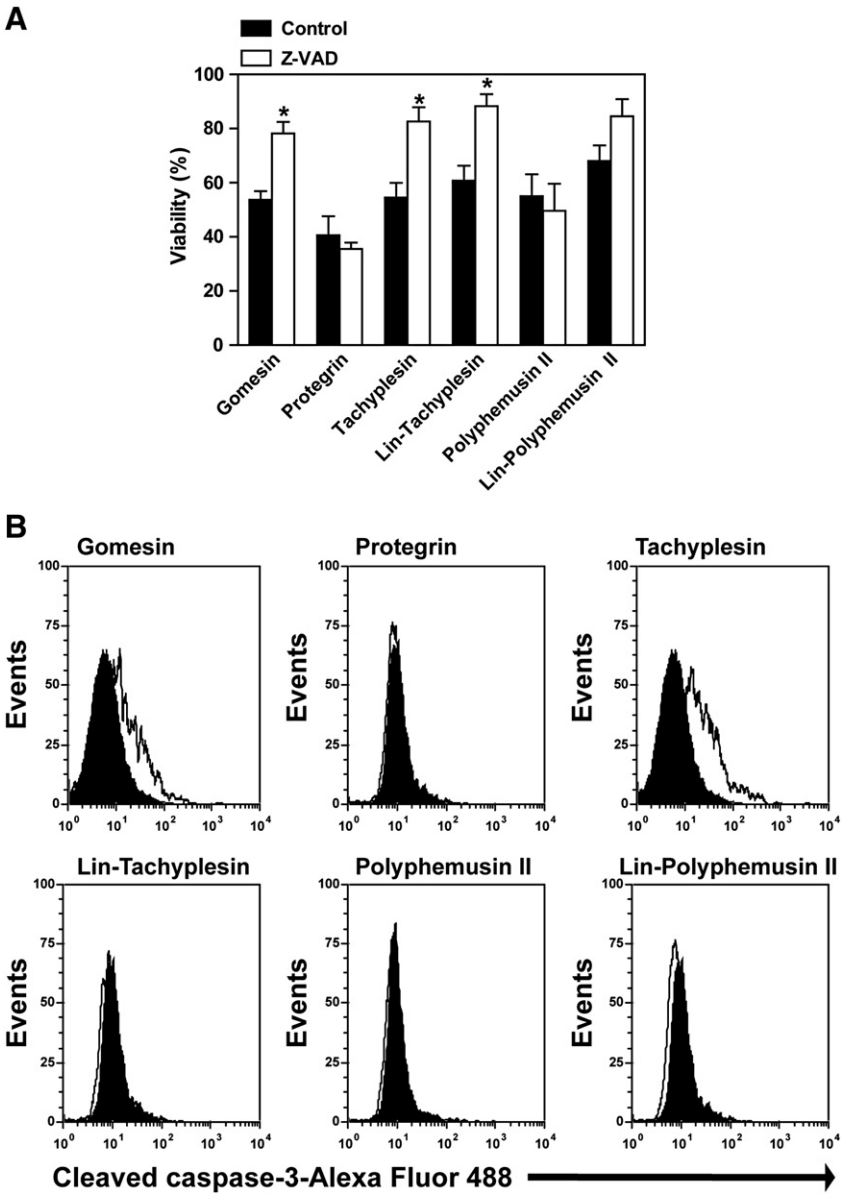

Fig. 3. Cell death induced by gomesin, tachyplesin and Lin-tachyplesin occurs by apoptosis. K562 cells were treated with each peptide at the cytotoxic EC_{50} for 24 h, and then evaluated. (A) Pretreatment of cells with 20 μM Z-VAD, a caspase inhibitor, decreased cell death induced by gomesin, tachyplesin and Lin-tachyplesin, whereas the effect of protegrin, polyphemusin and Lin-polyphemusin treatment on cell death was not altered. Results are the means ± SEM of three independent experiments performed in duplicate. *$P<0.05$, T-test. (B) Flow cytometric analysis of endogenous levels of activated caspase-3 in K562 cells. Filled and open histograms represent unstimulated and stimulated samples, respectively. Data are representative of three experiments.

Subsequently, nuclear analysis showed defragmented DNA in cells treated with all AMPs at the EC_{50} concentration (Fig. 4A). Quantification of cells with low DNA content (sub-diploid cells or sub-G_1/G_0) was performed by flow cytometry. Sub-diploid cells significantly but modestly increased with the use of all AMPs (Fig. 4B). Quantification of DNA content in cells treated with higher concentrations of AMPs was not possible because an extensive disruption of the cells was observed (data not shown).

The elicitation of intracellular oxidative stress is a characteristic of several cytotoxic agents [21–24]. Thus, free radicals were quantified using the CM-H_2DCFDA fluorophore. Among the AMPs, only protegrin led to a rise in free radicals after 24 h of treatment at the cytotoxic EC_{50} concentration for that AMP (Fig. 4C). The participation of free radicals in the cell death induced by protegrin was confirmed by the use of N-Acetyl-Cysteine (NAC), a thiol redox, which was able to inhibit cell death induced by protegrin (Fig. 4D). NAC could reduce the disulfide bridge in proteins [25], therefore the hypothesis of NAC to break the bridges of protegrin was tested. Protegrin and gomesin were incubated at different times with NAC, but no reduction of the peptide's bridges was observed by LC–MS (data not shown). In addition, NAC was not able to reduce the cytotoxic effect of gomesin (data not shown).

In addition, a necroptosis inhibitor, necrostatin-1, and an intracellular Ca^{2+} chelator, BAPTA-AM, were used. Necrostatin-1, a specific inhibitor of receptor-interacting protein 1 (RIP-1) kinase [26], inhibited induced cell death by gomesin, tachyplesin and Lin-polyphemusin II (Fig. 5A), while BAPTA-AM reduced the cell death promoted by gomesin and protegrin (Fig. 5B). Moreover, quantification of intracellular Ca^{2+} was assessed by confocal microscopy. We observed that gomesin and protegrin were able to induce an increase in Ca^{2+} levels in K562 cells, demonstrating that the Ca^{2+} ion participates in cell death induced by gomesin and protegrin (Fig. 5C).

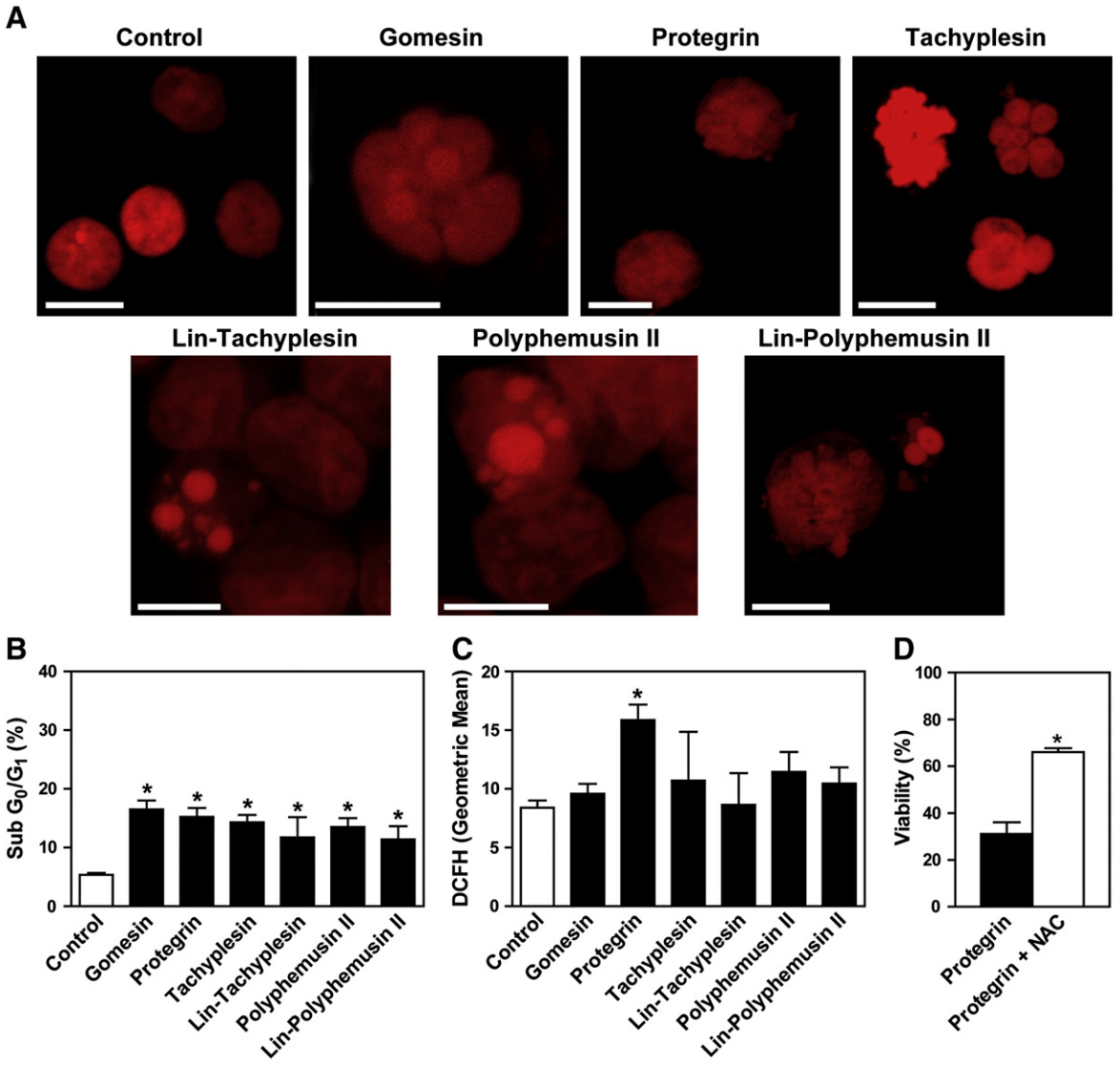

Fig. 4. Characterization of cell death induced by AMPs. K562 cells were treated with the EC_{50} of each peptide for 24 h, and then evaluated. (A) AMP-induced nuclear morphological features were visualized by confocal microscopy. Micrographs of control cells were stained with PI. Representative photomicrographs of two independent experiments are shown. Bars = 10 μm. (B) Measurement of cells with low DNA content performed by flow cytometry. (C) AMP-induced ROS generation was detected using the CM-H_2DCFDA fluorophore. (D) The cells were incubated for 1 h with NAC previously to stimulus. Then, 10 μM protegrin was added in the presence of NAC. Results are the means ± SEM of three independent experiments performed in duplicate. *$P<0.05$, ANOVA test.

3.2. High concentrations of AMPs induce direct cell membrane disruption

The evaluation of cell death by flow cytometry using higher concentrations of AMPs (above EC_{50} levels) revealed a second effect on cells by AMPs: cell membrane permeabilization (Supplementary material, Fig. S1). Representative contour plots showed the mode of cell death induced by AMPs using the cytotoxic EC_{50} concentration for each AMP or a concentration of 40 μM (Supplementary material, Fig. S1). All the AMPs that displayed cytotoxic activity induced cell death permeabilization at a concentration above the EC_{50}. The permeabilization of cell membranes was evidenced by PI uptake. The images in Fig. 6 allowed us to visualize details of membrane disruption upon treatment with AMPs for 24 h. A total disruption of the cell membrane was observed at high concentrations of gomesin. Treatment with tachyplesin and Lin-tachyplesin also led to a substantial alteration in the cell membrane, but some intact cells remained. Protegrin treatment produced rounding and swelling of cells, which is typical in necrotic cell death, and treatment with polyphemusin II and its linear analog also disrupted the cell membranes of K562 cells. However, treatment with magainin II, Lin-gomesin and Lin-protegrin, which possess low cytotoxic activity in K562 cells, did not promote visible alterations in the cell membranes. Light forward scatter and light side scatter, which correspond to size of cells and their granulation respectively, were quantified after treatment with AMPs (Supplementary material Fig. S2). All AMPs reduce the cell size after 24 h of treatment and the most of them, except tachyplesin and Lin-tachyplesin, promote increase of cell granulation likely by increase of density (Supplementary material, Fig. S2).

In addition, we analyzed the effect of treatment with 40 μM of AMPs on cell membranes using time-lapse capture in a light microscope. The time-lapse images revealed important differences of cell death induced by different AMPs. Gomesin induced some cellular swelling until a permeabilization in a specific area resulted in the release of the intracellular contents, and in some cases, membrane blebbing was observed (Supplementary material Fig. S3A). Protegrin induced cell death was different from that induced by the other AMPs. Protegrin induced an initial blebbing in all cells observed followed by high amplitude swelling of the cells (Supplementary

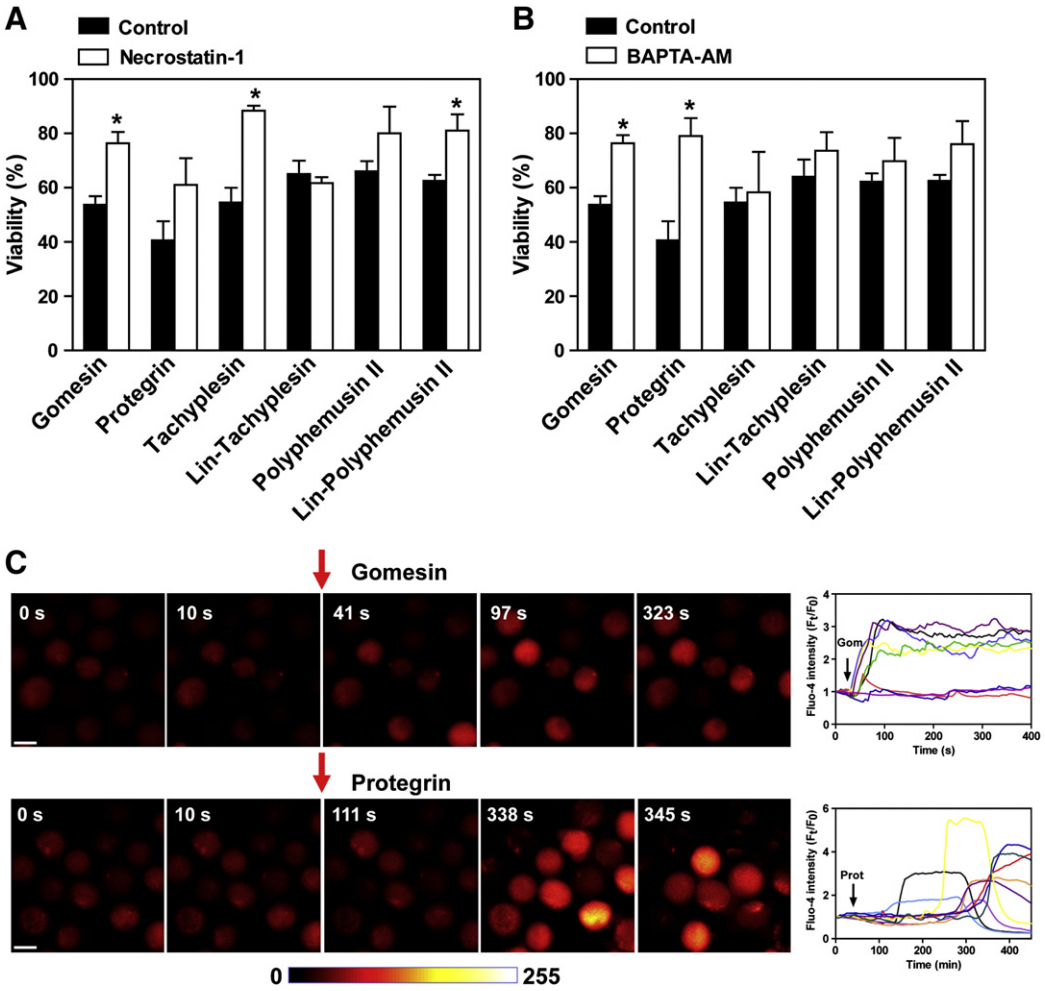

Fig. 5. Necroptotic cell death induced by AMPs and altered intracellular Ca^{2+} levels. K562 cells were treated with the EC_{50} of each peptide for 24 h, and then evaluated. (A) Pretreatment of cells with 20 μM necrostain-1, a RIP-1 kinase inhibitor, decreased cell death induced by gomesin, tachyplesin and Lin-polyphemusin, whereas the effect of treatment with protegrin, Lin-tachyplesin and polyphemusin on cell death was not altered. (B) Incubation of cells with 10 μM BAPTA-AM, an intracellular Ca^{2+} chelator, only decreased cell death in gomesin and protegrin treated cells. (C) Confocal images are shown using pseudocolor image according to a fluorescence intensity scale (0 = black, 255 = white). Representative images of basal $[Ca^{2+}]_i$ intensity and the intensity following protegrin and gomesin stimulation are shown. The records of fluorescence intensity as a function of time correspond to the images shown on the right. Each trace represents the temporal Fluo-4 fluorescence intensity of one cell. (A–B) Results are the means ± SEM of three independent experiments performed in duplicate. *P<0.05, T-test.

material Fig. S3B). Tachyplesin and its linear analog promoted membrane blebbing followed by swelling, which ultimately resulted in membrane disruption (Supplementary material Figs. S3C and S4A). Tachyplesin took the longest time of the AMPs to induce membrane disruption. Polyphemusin II promoted cell death started with small membrane blebbings and high amplitude swelling of the cells (Supplementary material Fig. S4B). Finally, Lin-polyphemusin II promotes a blebbing that increase by all extension of cell until the disruption of cell membrane (Fig. S4C). Using image software temporal alterations in cell shape, volume and blebbing were analyzed. The sequence of cell evaluation after stimulus with each peptide is shown in supplementary material (see Movies in supplementary material and Figs. S5–S10). Although AMPs induce rapid necrotic cell death with typical membrane permeabilization, it was possible to observe a diverse form of membrane alteration for each AMP. A common feature among them was the volume increase after stimulation. Polyphemusin II was the only AMP that did not promote blebbing formation leading directly to intracellular condensation and membrane permeabilization (Supplementary material, Fig. S9). For the other AMPs the blebbings appear in different numbers and a transient increase was observed, but after some minutes, with swelling formation, the blebbings are fused with the cell (Supplementary material, Fig. S5–S10).

Evaluation of cell membranes 24 h after treatment with AMPs at the EC_{50} concentration was performed by confocal microscopy. The cell membrane was labeled with WGA, a lectin that binds to N-acetylglucosamine [27]. A focal plane from the middle of the cells is shown in Fig. 7A. Control samples and cells stimulated with AMPs with low cytotoxic effects, such as magainin II, Lin-gomesin and Lin-protegrin, showed a homogeneous distribution of WGA labeling. In addition, AMPs that were cytotoxic to K562 cells caused accumulation of labeled WGA (Fig. 7A). Spatial evaluation of cells (control and gomesin treated cells were rotated 90° degrees) revealed a decrease in cell size after gomesin treatment, which explains the accumulation of WGA labeling observed (Fig. 7B).

Conversely, treatment with high concentrations of gomesin completely damaged the cell membrane (Fig. 7C). This explains the flow cytometry results in which all cells treated with gomesin stained positive for annexin and PI (Supplementary material Fig. S11A–B). Finally, the direct effect on cell membrane of gomesin was isolated decreasing cellular metabolism and performing cell death evaluation after 1 h. To decrease endocytosis of AMPs cell death curves were constructed at 4 °C or in the presence of cytochalasin D. Both treatments promote the shift of curve to right. The concentrations of 5–10 μM, which correspond to the range with apoptosis activity, were the most affected in these conditions. However, the effect of

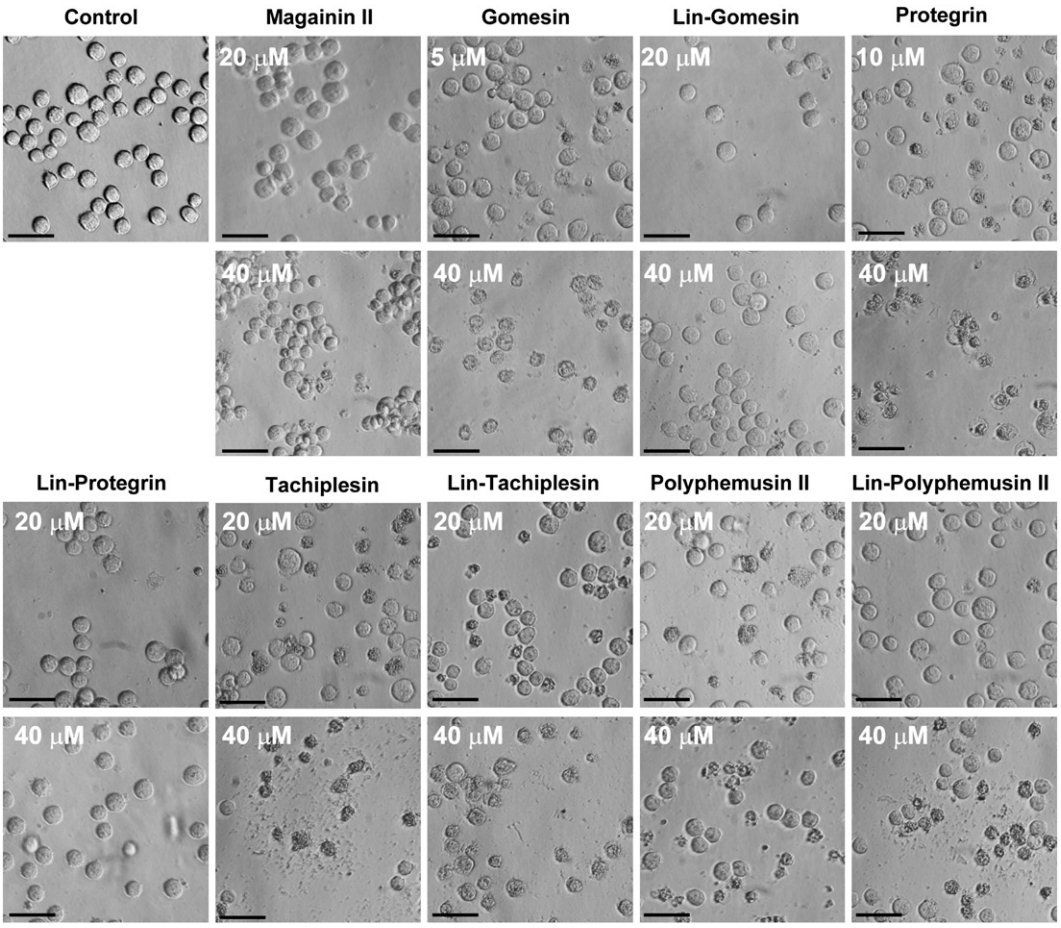

Fig. 6. Morphology of cells after treatment with AMPs. Photomicrographic observation of cell morphology was performed in cells treated with the cytotoxic EC_{50} or 40 μM of each peptide for 24 h. For magainin, Lin-gomesin and Lin-protegrin, a concentration of 20 μM was used. Bar = 25 μm.

concentration of 40 μM gomesin was not affected indicating that at this concentration the primarily effect occurs independent of cellular mechanism and occurs by a direct action of cell permeabilization.

4. Discussion

Several reports have described the antitumor activity of cationic AMPs; however, their specific mechanism of action in mammalian cells and its relation with their spatial structure remain unclear. Studies involving the intracellular mechanism of AMPs have revealed substantial differences in the manner in which AMPs induce cell death and in their preference to act on cancer or normal cells.

In this study, we investigated the capability of four β-hairpin AMPs, gomesin, protegrin, tachyplesin and polyphemusin II, and their corresponding linear analogs to induce cell death in K562 cells. Magainin II, an α-helix AMP, was also tested to compare the effects with the ones caused by the linear analogs. It was possible to distinguish diverse effects among these β-hairpin AMPs despite their structural similarities. We observed that the treatment with low concentrations of AMPs induced cell death by activation of several intracellular mechanisms, while treatment with high concentrations of AMPs induced rapid membrane disruption with diverse characteristics.

4.1. Differences in cell death mechanisms by AMPs at low concentration

Among the peptides used, magainin II exhibited the lowest cytotoxicity in K562 cells at concentrations below 40 μM, similar to what has been observed in other cell types [28–30]. Linear analogs of gomesin and protegrin also showed low cytotoxic activity (Fig. 1). However, linear counterparts of tachyplesin and polyphemusin did not exhibit a decrease in their cytotoxicity (Fig. 1). This suggests that the substitution of Cys by Ser, which leads to the assumption of α-helix secondary structures by peptides [31,32], is not enough to reduce the cytotoxic properties of these molecules. In general, Lin-tachyplesin and Lin-polyphemusin II acted similarly to their native molecules, as observed when their potency and efficacy were compared (Fig. 1 and Table 1). However, differences were found when the nature of cell death induced by tachyplesin, polyphemusin II and their corresponding counterparts were compared. Secondary necrosis, apoptosis and necrosis were induced to a similar extent by tachyplesin, whereas Lin-tachyplesin treatment showed a lower percentage of necrosis (Fig. 2). The cell death induced by both AMPs was reduced by treatment with Z-VAD, a caspase inhibitor (Fig. 3A). Another difference between Lin-tachyplesin and tachyplesin was that only tachyplesin was able to induce the cleavage of caspase-3 (Fig. 3A). Polyphemusin II induced mainly necrotic cell death, whereas its analog induced largely secondary necrosis (Fig. 2).

The differences observed in cellular responses to tachyplesin and polyphemusin II treatment are important because a high degree of homology exists between these AMPs (Table 1). Polyphemusin II and tachyplesin have the same seven amino acids residues at their C-termini strand. However, tachyplesin possesses two positive amino acids, Lys^1 and Arg^9, whereas polyphemusin II possesses three positive amino acids, Arg^1, Arg^2 and Lys^{10} (Table 1). In the strand N-termini a high degree of homology is also observed. The differences are the substitution of an Arg by a Lys and a Phe by an Ile (Table 1). The similarity between these two molecules can explain

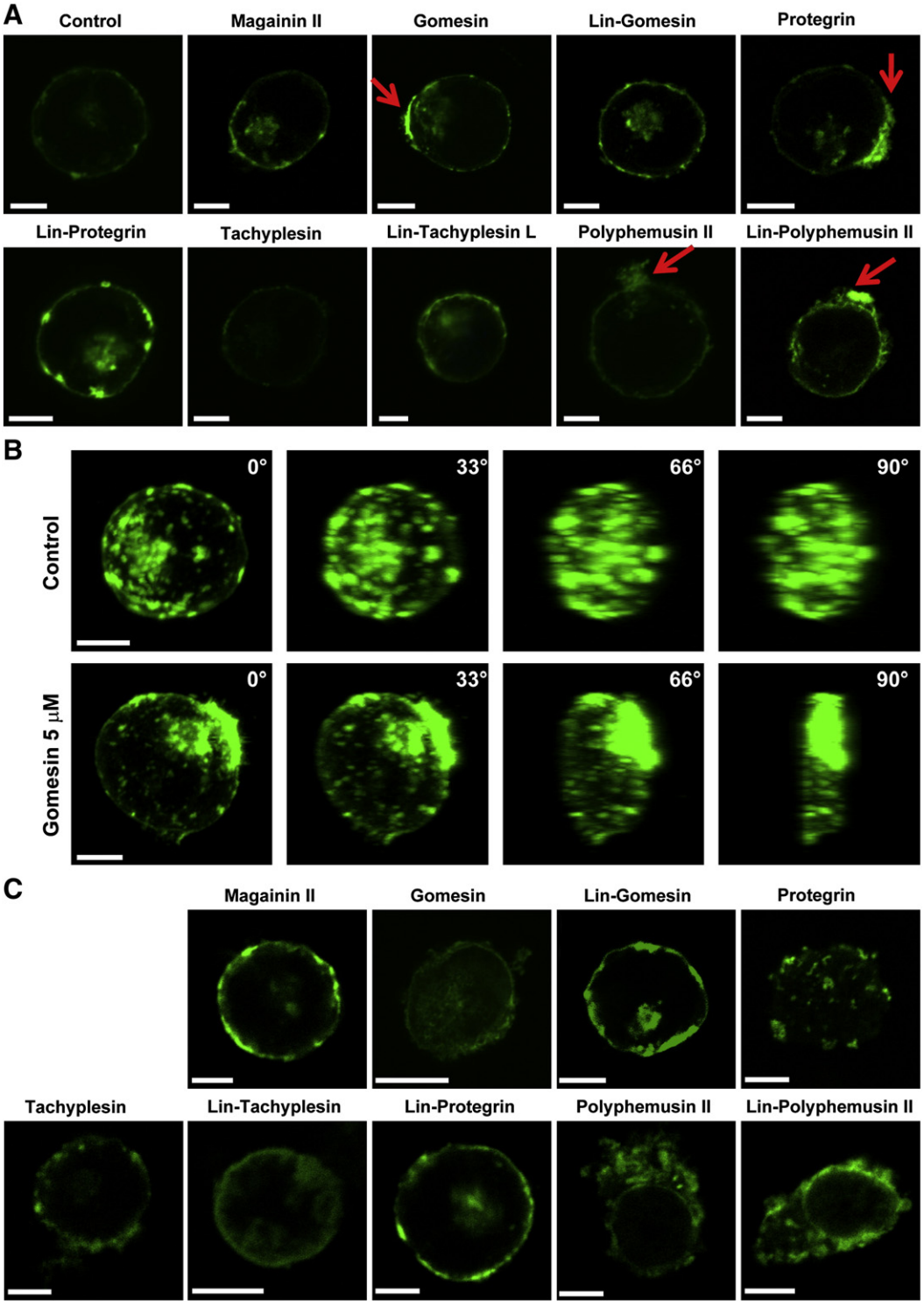

Fig. 7. Visual evaluation of cellular membranes after treatment with AMPs. Confocal images were captured in cells treated with the EC_{50} or 40 μM of each peptide for 24 h. A concentration of 20 μM was used for magainin, Lin-gomesin and Lin-protegrin. Bar = 5 μm. (A) The images shown are representative images of one focal plane. High levels of fluorescence (arrows) can be observed after incubation of cells with gomesin, protegrin, polyphemusin and Lin-polyphemusin. (B) Images in XY were acquired in a single confocal optical image, and a 3D image was constructed and rotated 90°. Images of control samples and cells stimulated with gomesin are shown. (C) The disruption of the cell membrane can be observed in cells treated with 40 μM of AMPs with cytotoxic ability.

why their linear analogs maintain their cytotoxic ability but does not explain the difference observed in the mechanism by which cell death is activated.

Gomesin and protegrin also have a partial homology. These AMPs have four similar amino acids (Arg-Leu-Cys-Tyr) in their C-termini, but gomesin has a larger amino acid chain in its N-terminus (Table 1). The linear analogs for both of these molecules lost their cytotoxic abilities. In addition, Ca^{2+} signaling participates in both gomesin and protegrin cell death-induction (Fig. 5B and C). Gomesin was the most potent AMP inducer of cell death of the AMPs and promoted apoptosis characterized by phosphatidylserine externalization and caspase-3 activation without cellular membrane permeabilization (Figs. 1B, 2A and 3B). However, in cancer cell lineages such as B16 melanoma [1], SH-SY5Y neuroblastoma and PC12

pheochromocytoma [14], gomesin has been shown to act mainly by Ca^{2+}-dependent membrane permeabilization [14]. As observed for gomesin and other AMPs, multiple cell death pathways were activated. Thus, apoptosis and necroptosis, both often dependent on Ca^{2+} signaling, could be activated simultaneously in K562 cells, explaining the inhibitory effect of Z-VAD and necrostatin-1 (Figs. 3A and 5A). This explanation could also extend to the inhibition of tachyplesin by necrostatin-1 (Fig. 5A). Conversely, necrosis was the primary type of cell death induced by protegrin, and it could only be inhibited by BAPTA, a Ca^{2+} chelator (Fig. 5B). In addition, protegrin was the only AMP that maintained high levels of free radicals for 24 h (Fig. 4C). The results related to cell death mechanism (Figs. 1–5) suggested that these β-hairpin AMPs did not produce a specific type of cell death, but they could activate several cell death mechanisms simultaneously.

4.2. Morphological differences observed in cell membrane by AMPs at high concentration

The effects observed with high concentrations of AMPs occur quickly (less than 20 min), unlike to other cytotoxic agents, and seem to primarily occur at the cell membrane (Fig. 6 and Fig. S1). It has been suggested that AMPs induce cell death by opening pores in cellular membranes, or that they possess a detergent-like effect resulting in membrane permeabilization [14,16,33–35]. Confocal evaluation of cell membranes showed alterations in membrane appearance when cells were treated with the EC_{50} concentration of the AMPs. However, the morphological integrity of the cell membranes appeared to remain (Fig. 7A). Spatial evaluation of cells after treatment with gomesin showed a reduction in cell volume when compared with control cells (Fig. 7B). Conversely, treatment with 40 μM of AMPs induced a major alteration in cellular structure, whereas treatment with magainin II, Lin-gomesin and Lin-protegrin did not alter cell appearance (Figs. 6 and 7C). Different changes in cell membrane integrity were observed for the different AMPs used (Fig. 7C).

Several models for the interaction of AMPs with membranes have been established such as barrel-stave, carpet or toroidal-pore models [36]. Although these models may be useful for understanding the actions of AMPs in bacteria or lipid vesicles, their relevance for understanding membrane disruption in mammalian cells need to be clarified. A comparison of cell membrane disruption by different AMPs also showed differences in membrane alterations. Temporal images shown here clearly support this hypothesis evidencing different kinds of membrane permeabilization, which deserves further investigation (see Movies in supplementary material).

Indeed morphological and volume evaluation of time-lapse images allowed to distinguish the diverse cell membrane permeabilization at high concentration by each β-hairpin AMP used in this study (Fig. S3–S10). Large differences in cell membrane permeabilization may be observed among structurally similar β-hairpin AMPs such as gomesin and protegrin, and tachyplesin and polyphemusin, or even between tachyplesin (or polyphemusin) and its linear counterpart.

It is believed that the main mode of action of these peptides on cell death in mammals' cells occurs through non-receptor mediated interactions with the external membrane because D-isoforms of AMPs are as cytotoxic as the native peptide [1,37,38]. Another theory that has been proposed to explain the action of these peptides relates to the cationic nature of most of these peptides. In this regard, electrostatic interactions between cationic AMPs and anionic cell membrane components are assumed to be a main feature in the interaction of AMPs with cancer cells [4,39–42]. Studies performed with negative and neutral bilayers have shown that protegrin and gomesin interact preferentially with negative bilayers compared to neutral bilayers that contain cholesterol [11,43]. This preference of AMPs for negative membranes over cholesterol containing membranes, such as mammalian cell membranes, explains the range of potency of AMPs in bacteria (0.1–2 μM), whereas in mammalian cells 10–50-fold (1–100 μM) higher concentrations of AMPs are necessary to induce membrane disruption [1,11,44].

4.3. Difference among the effects elicited by β-hairpin AMP

A possible explanation for the different cell death mechanisms triggered by β-hairpin AMPs at low concentration could be related to their interactions with extracellular molecules and cell membranes and their capacity to be endocytosed by the cells, as has been shown by several other reports [1,4,38,39]. It is possible that different AMPs may be targeted to different extracellular and intracellular structures to activate several cell death pathways. Given the negative charge of mitochondrial membranes and their structural similarity with bacteria membrane, it is possible that mitochondria are the preferential target for AMP leading to the activation of cell death such as apoptosis. Such a hypothesis is supported by studies that have shown that treatment with AMPs disrupts mitochondrial potential and other mitochondrial functions [28,45,46].

In contrast, the differences of cell membrane disruption at high concentration could be related to different interactions of AMPs with several components of cells such as extracellular matrix molecules and lipids, or with structural characteristics such as spatial conformation, hydrophobicity, and charge distribution.

Investigations that clarify the mode of action of AMPs are important, since they may impact on their potential development as antitumor agents. Although, the preference of AMPs by cancer cells is not clear, several reports show a highest cytotoxicity potency of AMPs against tumor cells than normal cells [2,47]. In a recent study, we only observed some differences of cytotoxicity potency of AMPs (gomesin, protegrin, tachyplesin and polyphemusin) when compared to normal mononuclear cells, K562 and HL-60, a human promyelocytic leukemia lineage, but some AMPs were able to affect these lineages with concentration that did not induce cell death, but inducing arrest of cell cycle and immunomodulation (unpublished results). As demonstrated in this study, even structurally similar AMPs can promote different effects at low and at high concentration [1,39]. Some reports have also shown similar effect of AMP between normal and cancer cells, therefore the relationship between AMP structure and activity is relevant to further explore the ability of these molecules against cancer cells, especially against resistant populations.

5. Conclusions

In this study we described diverse effects promoted by β-hairpin AMPs with similar tridimensional structures. We clearly distinguish between two biological effects promoted by β-hairpin AMPs at low and high concentration. We showed that despite of similar conformation these β-hairpin AMPs can promote activation of diverse intracellular mechanisms of cell death (at low concentration), and several forms of membrane disruption (at high concentration). In addition, by comparing AMPs to their linear analogs, we observed that linearization is not sufficient to reduce the cytotoxic ability of AMPs. In this study, controlled intracellular mechanism and direct membrane disruption were clearly distinguished for the first time helping to understand the real action of AMPs in mammalian cells.

Supplementary materials related to this article can be found online at doi:10.1016/j.bbagen.2012.02.015.

Acknowledgements

This study was supported by grants (to E. J. P-G and A.M.) from Fundação de Amparo à Pesquisa do Estado de São Paulo (FAPESP. Proc. 2009/54869-2, 2011/17584-0) and Conselho Nacional de

Desenvolvimento Científico e Tecnológico (CNPq). M. N. C. M. was supported by a PhD's fellowship from CAPES. A.M. was supported by grants from CNPq.

References

[1] E.G. Rodrigues, A.S. Dobroff, C.F. Cavarsan, T. Paschoalin, L. Nimrichter, R.A. Mortara, E.L. Santos, M.A. Fazio, A. Miranda, S. Daffre, L.R. Travassos, Effective topical treatment of subcutaneous murine B16F10-Nex2 melanoma by the antimicrobial peptide gomesin, Neoplasia 10 (2008) 61–68.

[2] M. Shi, H.N. Wang, S.T. Xie, Y. Luo, C.Y. Sun, X.L. Chen, Y.Z. Zhang, Antimicrobial peptaibols, novel suppressors of tumor cells, targeted calcium-mediated apoptosis and autophagy in human hepatocellular carcinoma cells, Mol. Cancer 9 (2010) 26.

[3] J.M. Ceron, J. Contreras-Moreno, E. Puertollano, G.A. de Cienfuegos, M.A. Puertollano, M.A. de Pablo, The antimicrobial peptide cecropin A induces caspase-independent cell death in human promyelocytic leukemia cells, Peptides 31 (2010) 1494–1503.

[4] J. Chen, X.M. Xu, C.B. Underhill, S. Yang, L. Wang, Y. Chen, S. Hong, K. Creswell, L. Zhang, Tachyplesin activates the classic complement pathway to kill tumor cells, Cancer Res. 65 (2005) 4614–4622.

[5] D.W. Hoskin, A. Ramamoorthy, Studies on anticancer activities of antimicrobial peptides, Biochim. Biophys. Acta 1778 (2008) 357–375.

[6] J.S. Mader, D.W. Hoskin, Cationic antimicrobial peptides as novel cytotoxic agents for cancer treatment, Expert Opin. Investig. Drugs 15 (2006) 933–946.

[7] N. Mandard, P. Bulet, A. Caille, S. Daffre, F. Vovelle, The solution structure of gomesin, an antimicrobial cysteine-rich peptide from the spider, Eur. J. Biochem. 269 (2002) 1190–1198.

[8] D. Bolintineanu, E. Hazrati, H.T. Davis, R.I. Lehrer, Y.N. Kaznessis, Antimicrobial mechanism of pore-forming protegrin peptides: 100 pores to kill *E. coli*, Peptides 31 (2010) 1–8.

[9] Y. Hirakura, S. Kobayashi, K. Matsuzaki, Specific interactions of the antimicrobial peptide cyclic beta-sheet tachyplesin I with lipopolysaccharides, Biochim. Biophys. Acta 1562 (2002) 32–36.

[10] D. Gidalevitz, Y. Ishitsuka, A.S. Muresan, O. Konovalov, A.J. Waring, R.I. Lehrer, K.Y. Lee, Interaction of antimicrobial peptide protegrin with biomembranes, Proc. Natl. Acad. Sci. U. S. A. 100 (2003) 6302–6307.

[11] R. Mani, S.D. Cady, M. Tang, A.J. Waring, R.I. Lehrer, M. Hong, Membrane-dependent oligomeric structure and pore formation of a beta-hairpin antimicrobial peptide in lipid bilayers from solid-state NMR, Proc. Natl. Acad. Sci. U. S. A. 103 (2006) 16242–16247.

[12] L. Cruz-Chamorro, M.A. Puertollano, E. Puertollano, G.A. de Cienfuegos, M.A. de Pablo, In vitro biological activities of magainin alone or in combination with nisin, Peptides 27 (2006) 1201–1209.

[13] H.T. Zhang, J. Wu, H.F. Zhang, Q.F. Zhu, Efflux of potassium ion is an important reason of HL-60 cells apoptosis induced by tachyplesin, Acta Pharmacol. Sin. 27 (2006) 1367–1374.

[14] R.C. Soletti, L. del Barrio, S. Daffre, A. Miranda, H.L. Borges, V. Moura-Neto, M.G. Lopez, N.H. Gabilan, Peptide gomesin triggers cell death through L-type channel calcium influx, MAPK/ERK, PKC and PI3K signaling and generation of reactive oxygen species, Chem. Biol. Interact. 186 (2010) 135–143.

[15] S.J. DeMarco, H. Henze, A. Lederer, K. Moehle, R. Mukherjee, B. Romagnoli, J.A. Robinson, F. Brianza, F.O. Gombert, S. Lociuro, C. Ludin, J.W. Vrijbloed, J. Zumbrunn, J.P. Obrecht, D. Obrecht, V. Brondani, F. Hamy, T. Klimkait, Discovery of novel, highly potent and selective beta-hairpin mimetic CXCR4 inhibitors with excellent anti-HIV activity and pharmacokinetic profiles, Bioorg. Med. Chem. 14 (2006) 8396–8404.

[16] M.A. Fazio, V.X. Oliveira Jr., P. Bulet, M.T. Miranda, S. Daffre, A. Miranda, Structure–activity relationship studies of gomesin: importance of the disulfide bridges for conformation, bioactivities, and serum stability, Biopolymers 84 (2006) 205–218.

[17] E.J. Paredes-Gamero, C.M. Leon, R. Borojevic, M.E. Oshiro, A.T. Ferreira, Changes in intracellular Ca^{2+} levels induced by cytokines and P2 agonists differentially modulate proliferation or commitment with macrophage differentiation in murine hematopoietic cells, J. Biol. Chem. 283 (2008) 31909–31919.

[18] C.M. Barbosa, C.M. Leon, A. Nogueira-Pedro, F. Wasinsk, R.C. Araujo, A. Miranda, A.T. Ferreira, E.J. Paredes-Gamero, Differentiation of hematopoietic stem cell and myeloid populations by ATP is modulated by cytokines, Cell Death Dis. 2 (2011) e165.

[19] I. Vermes, C. Haanen, H. Steffens-Nakken, C. Reutelingsperger, A novel assay for apoptosis. Flow cytometric detection of phosphatidylserine expression on early apoptotic cells using fluorescein labelled Annexin V, J. Immunol. Methods 184 (1995) 39–51.

[20] W.C. Earnshaw, L.M. Martins, S.H. Kaufmann, Mammalian caspases: structure, activation, substrates, and functions during apoptosis, Annu. Rev. Biochem. 68 (1999) 383–424.

[21] T.V. Berghe, N. Vanlangenakker, E. Parthoens, W. Deckers, M. Devos, N. Festjens, C.J. Guerin, U.T. Brunk, W. Declercq, P. Vandenabeele, Necroptosis, necrosis and secondary necrosis converge on similar cellular disintegration features, Cell Death Differ. 17 (2010) 922–930.

[22] H. Goto, H. Takahashi, H. Fujii, K. Ikuta, S. Yokota, N-(4-Hydroxyphenyl)retinamide (4-HPR) induces leukemia cell death via generation of reactive oxygen species, Int. J. Hematol. 78 (2003) 219–225.

[23] L. Yi, X.X. Ji, M. Lin, H. Tan, Y. Tang, L. Wen, Y.H. Ma, Q. Su, Diallyl disulfide induces apoptosis in human leukemia HL-60 cells through activation of JNK mediated by reactive oxygen, Pharmazie 65 (2010) 693–698.

[24] H.F. Lu, S.C. Hsueh, Y.T. Ho, M.C. Kao, J.S. Yang, T.H. Chiu, S.Y. Huamg, C.C. Lin, J.G. Chung, ROS mediates baicalin-induced apoptosis in human promyelocytic leukemia HL-60 cells through the expression of the Gadd153 and mitochondrial-dependent pathway, Anticancer Res. 27 (2007) 117–125.

[25] F.M. Rubino, M. Pitton, E. Caneva, M. Pappini, A. Colombi, Thiol-disulfide redox equilibria of glutathione metaboloma compounds investigated by tandem mass spectrometry, Rapid Commun. Mass Spectrom. 22 (2008) 3935–3948.

[26] A. Degterev, J. Hitomi, M. Germscheid, I.L. Ch'en, O. Korkina, X. Teng, D. Abbott, G.D. Cuny, C. Yuan, G. Wagner, S.M. Hedrick, S.A. Gerber, A. Lugovskoy, J. Yuan, Identification of RIP1 kinase as a specific cellular target of necrostatins, Nat. Chem. Biol. 4 (2008) 313–321.

[27] G. Bains, R.T. Lee, Y.C. Lee, E. Freire, Microcalorimetric study of wheat germ agglutinin binding to N-acetylglucosamine and its oligomers, Biochemistry 31 (1992) 12624–12628.

[28] S. Liu, H. Yang, L. Wan, H.W. Cai, S.F. Li, Y.P. Li, J.Q. Cheng, X.F. Lu, Enhancement of cytotoxicity of antimicrobial peptide magainin II in tumor cells by bombesin-targeted delivery, Acta Pharmacol. Sin. 32 (2011) 79–88.

[29] J. Lehmann, M. Retz, S.S. Sidhu, H. Suttmann, M. Sell, F. Paulsen, J. Harder, G. Unteregger, M. Stockle, Antitumor activity of the antimicrobial peptide magainin II against bladder cancer cell lines, Eur. Urol. 50 (2006) 141–147.

[30] R.A. Cruciani, J.L. Barker, M. Zasloff, H.C. Chen, O. Colamonici, Antibiotic magainins exert cytolytic activity against transformed cell lines through channel formation, Proc. Natl. Acad. Sci. U. S. A. 88 (1991) 3792–3796.

[31] L.G.M. Moraes, M.A. Fazio, R.F.F. Vieira, C.R. Nakaie, M.T.M. Miranda, S. Schreier, S. Daffre, A. Miranda, Conformational and functional studies of gomesin analogues by CD, EPR and fluorescence spectroscopies, Biochim. Biophys. Acta, Biomembr. 1768 (2007) 52–58.

[32] M.A. Fazio, L. Jouvensal, F. Vovelle, P. Bulet, M.T. Miranda, S. Daffre, A. Miranda, Biological and structural characterization of new linear gomesin analogues with improved therapeutic indices, Biopolymers 88 (2007) 386–400.

[33] L.G. Moraes, M.A. Fazio, R.F. Vieira, C.R. Nakaie, M.T. Miranda, S. Schreier, S. Daffre, A. Miranda, Conformational and functional studies of gomesin analogues by CD, EPR and fluorescence spectroscopies, Biochim. Biophys. Acta 1768 (2007) 52–58.

[34] M. Schaeffer, A. de Miranda, J.C. Mottram, G.H. Coombs, Differentiation of *Leishmania major* is impaired by over-expression of pyroglutamyl peptidase I, Mol. Biochem. Parasitol. 150 (2006) 318–329.

[35] C.K. Moreira, F.G. Rodrigues, A. Ghosh, P. Varotti Fde, A. Miranda, S. Daffre, M. Jacobs-Lorena, L.A. Moreira, Effect of the antimicrobial peptide gomesin against different life stages of *Plasmodium* spp, Exp. Parasitol. 116 (2007) 346–353.

[36] K.A. Brogden, Antimicrobial peptides: pore formers or metabolic inhibitors in bacteria? Nat. Rev. Microbiol. 3 (2005) 238–250.

[37] T. Iwasaki, J. Ishibashi, M. Kubo, D. Taylor, M. Yamakawa, Multiple functions of short synthetic enantiomeric peptides based on beetle defensins, Biosci. Biotechnol. Biochem. 73 (2009) 683–687.

[38] N. Papo, A. Braunstein, Z. Eshhar, Y. Shai, Suppression of human prostate tumor growth in mice by a cytolytic D-, L-amino acid peptide: membrane lysis, increased necrosis, and inhibition of prostate-specific antigen secretion, Cancer Res. 64 (2004) 5779–5786.

[39] B. Fadnes, O. Rekdal, L. Uhlin-Hansen, The anticancer activity of lytic peptides is inhibited by heparan sulfate on the surface of the tumor cells, BMC Cancer 9 (2009) 183.

[40] J. Wang, D.L. Rabenstein, Interaction of heparin and heparin-derived oligosaccharides with synthetic peptide analogues of the heparin-binding domain of heparin/heparan sulfate-interacting protein, Biochim. Biophys. Acta 1790 (2009) 1689–1697.

[41] H. Schroder-Borm, R. Bakalova, J. Andra, The NK-lysin derived peptide NK-2 preferentially kills cancer cells with increased surface levels of negatively charged phosphatidylserine, FEBS Lett. 579 (2005) 6128–6134.

[42] A. Risso, M. Zanetti, R. Gennaro, Cytotoxicity and apoptosis mediated by two peptides of innate immunity, Cell. Immunol. 189 (1998) 107–115.

[43] T.M. Domingues, K.A. Riske, A. Miranda, Revealing the lytic mechanism of the antimicrobial peptide gomesin by observing giant unilamellar vesicles, Langmuir 26 (2010) 11077–11084.

[44] P.I. Silva Jr., S. Daffre, P. Bulet, Isolation and characterization of gomesin, an 18-residue cysteine-rich defense peptide from the spider *Acanthoscurria gomesiana* hemocytes with sequence similarities to horseshoe crab antimicrobial peptides of the tachyplesin family, J. Biol. Chem. 275 (2000) 33464–33470.

[45] E.J. Helmerhorst, P. Breeuwer, W. van't Hof, E. Walgreen-Weterings, L.C. Oomen, E.C. Veerman, A.V. Amerongen, T. Abee, The cellular target of histatin 5 on *Candida albicans* is the energized mitochondrion, J. Biol. Chem. 274 (1999) 7286–7291.

[46] C. Segura, F. Guzman, L.M. Salazar, M.E. Patarroyo, S. Orduz, V. Lemeshko, BTM-P1 polycationic peptide biological activity and 3D-dimensional structure, Biochem. Biophys. Res. Commun. 353 (2007) 908–914.

[47] K. Okumura, A. Itoh, E. Isogai, K. Hirose, Y. Hosokawa, Y. Abiko, T. Shibata, M. Hirata, H. Isogai, C-terminal domain of human CAP18 antimicrobial peptide induces apoptosis in oral squamous cell carcinoma SAS-H1 cells, Cancer Lett. 212 (2004) 185–194.